Progress In Electromagnetics Research, PIER 10, 41–74, 1995

THE SPECTRAL INDEX METHOD FOR SEMICONDUCTOR RIB AND RIDGE WAVEGUIDES

S. V. Burke

1. Introduction

The Spectral Index (SI) method [1–9] is a fast and accurate semi-analytical technique. It was introduced in 1989 to analyze specifically waveguides of the type depicted in Figure 1. These include the familiar rib and ridge waveguide and also more general multilayered structures. These types of waveguide are important, of course, for they form the basis of numerous optoelectronic devices. Each structure consists of essentially a planar slab waveguide, cladded by air where the layer or layers adjacent to air have been etched to form a rib in order to laterally confine the propagating modes.

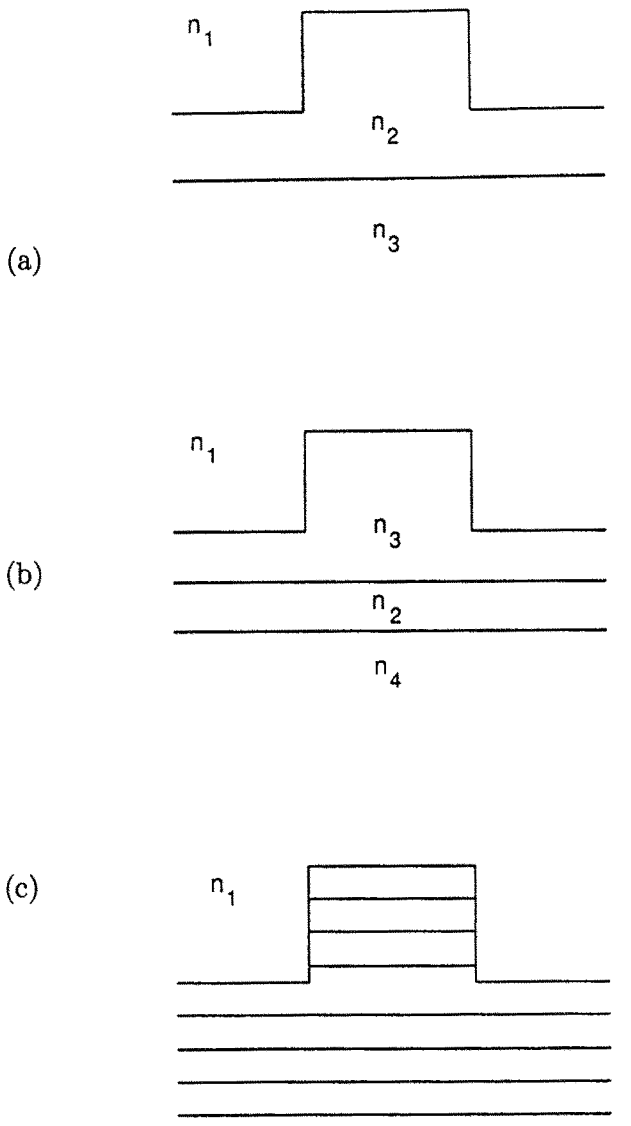

Figure 1. Cross-section through (a) rib waveguide (b) ridge waveguide (c) multilayered rib waveguide. Refractive indices of layers in (a) and (b) are related by $n_1 < n_4 \leq n_3 < n_2$ where n_1 corresponds to air. Refractive indices of layers in (c) are of arbitrary value.

The SI method relies on and takes advantage of both the low refractive index of the cladding (air) in these structures and their asymmetric but regular geometry. For analysis, the waveguides are divided into three regions (Figure 2). Each region is incorporated into the model in a separate way. In region I, the cladding, following a slight modification of the boundaries using the method of false position (Figure 3), the field is set to zero. In region II, the rib, and independently in region Ill, the system of layers beneath the rib, the polarized wave equation is solved exactly. A separable solution is chosen in region II whereas a Fourier approach is selected in region III. To link these solutions across the base of the rib a variational boundary condition is employed. This gives rise to a transcendental equation whose numerical solution gives the propagation constants of both quasi-TE and quasi-TM modes.

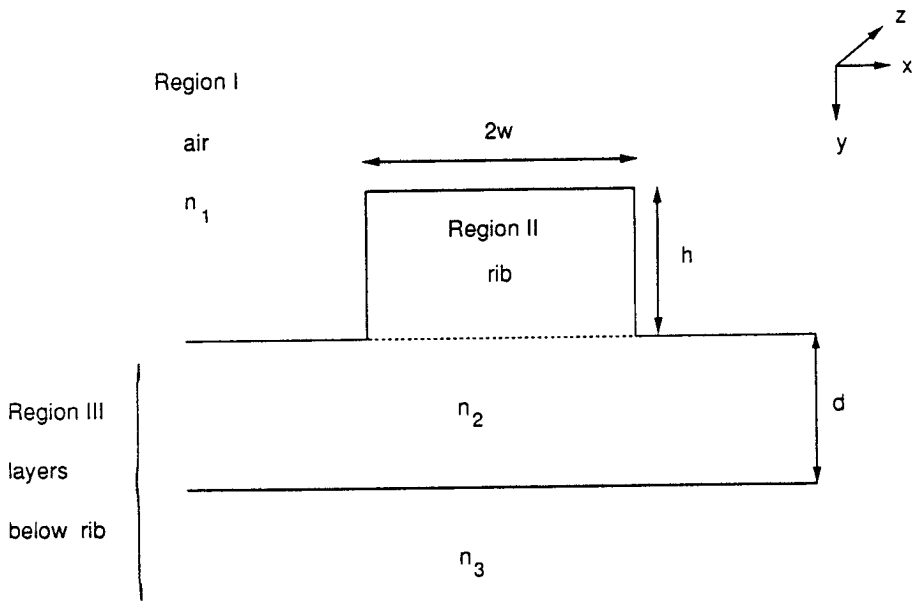

Figure 2. Cross-section through a rib waveguide divided into 3 regions for analysis by the SI method.

The calculated propagation constants and modal field profiles compare well with those produced by large-scale numerical techniques such as the finite difference [10–12] and finite element [13] methods. The SI method, however, typically requires only about 1% of the CPU time used by these other techniques, making it suitable for implementation on a desktop PC. The SI method is therefore the first rib waveguide modeling method to bridge the gap between highly accurate numerical methods (mentioned above) and simple, less accurate, intuitive approaches such as the effective index method [14] and the recently improved weighted index method [15], described elsewhere in this volume.

Since its discovery, the SI method has been continuously revised and extended. In particular, the SI method has been adapted to model both symmetric [16,17] and asymmetric [18] couplers, generating the propagation constants of the two-dimensional supermodes. Recently, a fully complex version of the method has been developed in order to model structures incorporating both gain and loss [19]. The SI method is thus an efficient design tool for a wide range of optoelectronic devices including, for example, wavelength demultiplexers [20–22] and laser amplifiers [23,24].

We begin in section 2 with a detailed description of the SI method as applied to the simplest case, the single rib waveguide. In section 3 we show how the SI method can be extended to model symmetric couplers and include a brief discussion on its adaptation to asymmetric couplers where the ribs can be of different composition and geometry. The discrete SI method [25], an alternative form which permits the rapid evaluation of overlap integrals, is dealt with in section 4 and finally section 5 is devoted to the adaptation of the SI method to structures with complex refractive indices.

2. The Symmetric Single Rib Waveguide

We consider the even and odd modes of the single rib waveguide illustrated in Figure 2. The structure and nomenclature are also shown. The guide consists of a substrate of index n_3 and guide layer of index n_2 which has been etched to form a rib of width $2w$ and height h leaving a lateral layer of thickness d. The cladding of index n_1 is assumed to be air. The structure is divided into three regions for analysis

namely the cladding, the rib and the layered region below the rib. The even modes will be considered first.

We begin with the wave equation in the form:

$$\partial^2 E/\partial x^2 + \partial^2 E/\partial y^2 + [k^2(x,y) - \beta^2]E = 0 \tag{1}$$

We solve for either even quasi-TE or even quasi-TM modes by choosing E to represent the principal field component in each case i.e. either E_x or E_y respectively and applying the appropriate boundary conditions. Here the x-axis is horizontal and the y-axis is vertical as shown in Figure 2. In (1), $k(x,y) = k_0 n(x,y)$ where k_0 is the wavenumber in free-space, and $n(x,y)$ is the refractive index profile in the cross-section of the waveguide, in a plane perpendicular to the direction of propagation, z. We have assumed the mode to have a z-dependency of the form $\exp(-j\beta z)$ where β is the propagation constant.

We begin by describing separately the treatment in each of the three regions and finding solutions to (1) independently in regions II and III. We then match these solutions across the base of the rib to form a transcendental equation for β.

2.1 Region I: The Cladding

Most semiconductor compounds of interest in optoelectronics have refractive indices significantly greater than that of air, for example the refractive index of GaAs is $\cong 3.4$. The SI method exploits this fact by setting the field to zero outside the semiconductor. However, to allow for the slight penetration of field into the cladding the boundaries are shifted slightly using the method of false position. This in fact involves making small additions to d, h and w forming effective values D, H and W. The additions required depend upon the orientation of the field component relative to the boundary concerned and have been derived by Kendall (chapter 2 in [7]).

For a field component orientated normally to an interface the virtual position of the interface should be moved a distance Δ_n into the cladding where

$$\Delta_n = \frac{n_1^2}{n_2^2} \frac{1}{(\beta^2 - k_1^2)^{1/2}} \tag{2}$$

and

$$k_1^2 = n_1^2 k_0^2.$$

Similarly, for a field component orientated tangentially to an interface the movement required along the normal is Δ_t where

$$\Delta_t = 1/(\beta^2 - k_1^2)^{1/2} \tag{3}$$

We therefore obtain the following relationships

$$\left.\begin{aligned} W &= w + \Delta_n \\ H &= h \\ D &= d + \Delta_t \end{aligned}\right\} \tag{4}$$

for quasi-TE modes and

$$\left.\begin{aligned} W &= w + \Delta_t \\ H &= h \\ D &= d + \Delta_n \end{aligned}\right\} \tag{5}$$

for quasi-TM modes. We note that for this case, the rib waveguide, the net height of the rib remains unaltered. The effective values, D, H and W are used throughout the subsequent analysis.

We see that for semiconductors with refractive indices of about 3 and for a wavelength of about $1.0\mu m$, Δ_t is approximately $0.05\mu m$ an Δ_n is roughly 10 times smaller than that. To aid computation, because of course β is not known in advance, β in (2) and (3) can therefore be replaced with $k_0 n_3$, with no significant loss of accuracy.

The implementation of the method of false position is illustrated in Figure 3, along with the coordinate system used in this analysis. We note that the origin is placed in the center of the rib on a line coincident with the displaced semiconductor/air boundary.

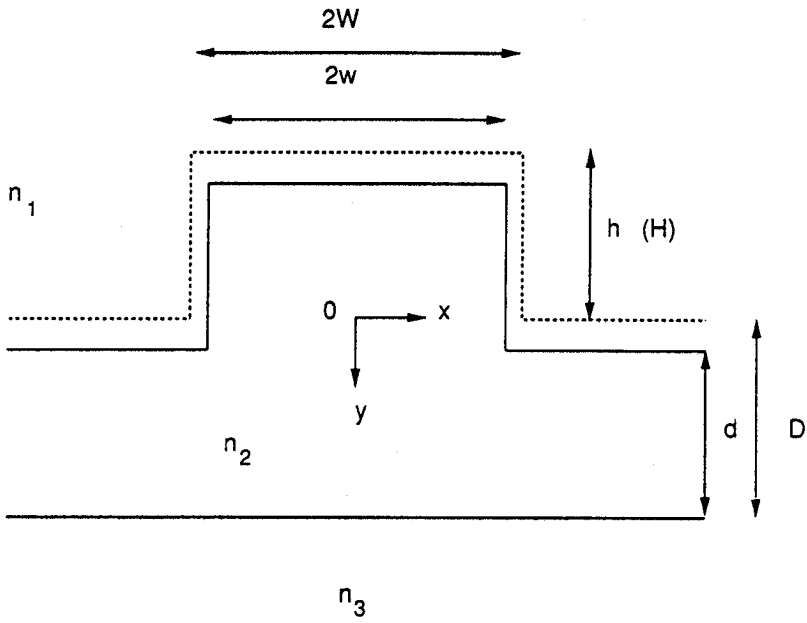

Figure 3. Illustration of the method of false position. The real dimensions d, h and w are transposed to their effective values D, H and W. The origin is located on a line coincident with the displaced semiconductor/air boundary.

2.2 Region II: The Rib

In the rib we take E (representing either E_x or E_y for even quasi-TE or even quasi-TM modes respectively) to be of the form

$$E = \sum_{m=1}^{\infty} A_m F_m(x) G_m(y) \tag{6}$$

where

$$F_m(x) = \cos\left[\frac{(2m-1)}{2W}\pi x\right] \tag{7}$$

and A_m are coefficients. It has been verified in [6] that apart for the case of modes very close to cut-off it is necessary to retain only the first term in this series. We can therefore write E in the form of a separable solution in x and y

$$E = F(x)G(y) \tag{8}$$

where for even modes

$$F(x) = \cos(s_1 x) \tag{9}$$

and $s_1 = \pi/2W$, greatly simplifying the analysis. We note that $F(x)$ is zero at $x = \pm W$.

If we substitute $E = G(y)\cos(s_1 x)$ into the scalar wave equation (1) we obtain

$$\partial^2 G(y)/\partial y^2 + (k^2 - \beta^2 - s_1^2)G(y) = 0 \tag{10}$$

which has solutions of the form

$$G(y) = \frac{\sin(\gamma_1(y+H))}{\sin(\gamma_1 H)} \tag{11}$$

where

$$\gamma_1 = (k_2^2 - s_1^2 - \beta^2)^{1/2}$$

and

$$k_2 = k_0 n_2$$

The expression for $G(y)$ above is normalized for convenience so that E assumes a value of unity at the origin. For large rib widths and/or low indices, γ_1 can become imaginary and (11) is then replaced by its hyperbolic form. From (8), (9) and (11) our final expression for E in the rib becomes

$$E(x,y) = \cos(s_1 x)\frac{\sin(\gamma_1(y+H))}{\sin(\gamma_1 H)} \tag{12}$$

2.3 Region III: Below the Rib

Below the rib we take the Fourier transform of E such that

$$\phi(s,y) = \int_{-\infty}^{+\infty} E(x,y)e^{jsx}dx \tag{13}$$

and

$$E(x,y) = \int_{-\infty}^{+\infty} \phi(s,y)e^{-jsx}dx \tag{14}$$

where s is a spatial spectral variable. By substituting (14) into (1) we obtain

$$\partial^2\phi(s,y)/\partial y^2 + \left\{k^2(y) - s^2 - \beta^2\right\}\phi(s,y) = 0 \tag{15}$$

We see that the x-dependency of the problem has been removed and the solution to (15) is equivalent to that of a planar slab but with layers having "spectral" indices n_s where

$$n_s = (n^2 - s^2/k_0^2)^{1/2} \tag{16}$$

We can write down expressions for ϕ in both the guide layer and substrate respectively such that

$$\phi(s,y) = A\sin\{\Gamma_2(y-D)\} + B\cos\{\Gamma_2(y-D)\} \qquad 0 < y > D \tag{17}$$

and

$$\phi(s,y) = C\exp\{-\Gamma_3(y-D)\} \qquad y > D \tag{18}$$

where A, B and C are coefficients. Also

$$\Gamma_2 = (k_2^2 - \beta^2 - s^2)^{1/2}$$

and

$$\Gamma_3 = (\beta^2 + s^2 - k_3^2)^{1/2}$$

2.4 Construction of the Transcendental Equation

We now have solutions to the scalar wave equation in the rib and independently in the layered region below the rib. We must now match these solutions along the base of the rib with suitable boundary conditions to obtain a transcendental equation for β. We use the subscripts + and - to denote a solution derived from just below (y is positive) and just above (y is negative) the interface respectively. Thus on the base of the rib

$$E_+ = E_- \tag{19}$$

However, $(\partial E/\partial y)_+$ is not necessarily equal to $(\partial E/\partial y)_-$. We therefore replace the usual condition of continuity of $\partial E/\partial y$ by the continuous stored power condition [26]. This is variational and should result in the most accurate values of β obtainable. The expression ψ is made stationary where

$$\psi = \int_{-\infty}^{+\infty} E^*[\partial E/\partial y]dx \tag{20}$$

Here * denotes the complex conjugate (of only those complex numbers arising from the Fourier transform) and $[\partial E/\partial y]$ is the increment in $\partial E/\partial y$ evaluated either side of $y = 0$. Equation (20) can be derived directly from the scalar wave equation. A detailed description of this procedure is provided by McIlroy (chapter 5 in [7]). The corresponding vector form is thoroughly discussed by Jones (chapter 3 in [7]). It can be shown that (20) is equally valid, with the appropriate field component, for both TE and TM modes.

Applying (20) to the current analysis, letting ψ tend to zero, and noting that the field is zero in the cladding we can write

$$\int_{-W}^{W} E_-^*(\partial E/\partial y)_- dx = \frac{1}{2\pi}\int_{-\infty}^{+\infty} \phi_+^*(\partial\phi/\partial y)_+ ds \tag{21}$$

Here, we have employed a Parseval-type formula of the form

$$\int_{-\infty}^{+\infty} PQ^* dx = \frac{1}{2\pi}\int_{-\infty}^{+\infty} \tilde{P}\tilde{Q}^* ds \tag{22}$$

where $\tilde{P}$ and $\tilde{Q}$ are the Fourier transforms of P and Q.

The left hand side of (21) is constructed just inside the rib while the right hand side is constructed just below the rib. Beginning with the left hand side we can determine E_- and $(\partial E/\partial y)_-$ from (12):

$$E_- = \cos(s_1 x) \tag{23}$$

and

$$(\partial E/\partial y)_- = \cos(s_1 x)\gamma_1 \cot(\gamma_1 H) \tag{24}$$

Substituting (23) and (24) into (21) and integrating over the width of the rib we find

$$\int_{-W}^{+W} E_-^*(\partial E/\partial y)_- dx = W\gamma_1 \cot(\gamma_1 H) \tag{25}$$

We can rewrite the right hand side of (21) in the form

$$\frac{1}{2\pi}\int_{-\infty}^{+\infty} \phi_+^*(\partial\phi/\partial y)_+ ds = \frac{1}{2\pi}\int_{-\infty}^{+\infty} \Gamma\phi_+\phi_+^* ds \tag{26}$$

where Γ has been defined as

$$\Gamma = \frac{(\partial\phi/\partial y)_+}{\phi_+} \tag{27}$$

Both ϕ_+ and $(\partial\phi/\partial y)_+$ are derived from (17) and (18) by matching the field solutions at $y = D$ with the usual dielectric slab boundary conditions. We find

$$\phi_+ = C\{\cos(\Gamma_2 D) + \Gamma_3 \sin(\Gamma_2 D)/\Gamma_2\} \tag{28}$$

and

$$(\partial\phi/\partial y)_+ = C\{\Gamma_2 \sin(\Gamma_2 D) - \Gamma_3 \cos(\Gamma_2 D)\} \tag{29}$$

These expressions apply for both quasi-TE and quasi-TM modes if for quasi-TM modes we multiply Γ_3 by the prefactor $m_1 = k_2^2/k_3^2$. Thus from (27), (28) and (29) Γ is given in full by

$$\Gamma = \Gamma_2 \frac{\Gamma_2 \sin(\Gamma_2 D) - \Gamma_3 \cos(\Gamma_2 D)}{\Gamma_2 \cos(\Gamma_2 D) + \Gamma_3 \sin(\Gamma_2 D)} \tag{30}$$

We note that Γ depends entirely on the form of the layered region below the rib. To complete the right hand side of (21) we take the Fourier transform of E_- in (23) (forming ϕ_-) noting that the field is set to zero in the cladding so that

$$\phi_- = \int_{-W}^{+W} \cos(s_1 x) e^{jsx} dx \tag{31}$$

We are dealing with an even function in x so this simplifies to

$$\phi_- = \int_{-W}^{+W} \cos(s_1 x) \cos(sx) dx \tag{32}$$

The integral in (32) is easily evaluated analytically so that

$$\phi_- = \frac{2s_1 \cos(sW)}{(s_1^2 - s^2)} \tag{33}$$

From (21), (25), (26) and (33) we construct the final transcendental equation for the even modes of a single rib waveguide:

$$\gamma_1 \cot(\gamma_1 H) = \frac{2}{\pi} \frac{s_1^2}{W} \int_{-\infty}^{+\infty} \Gamma \frac{\cos^2(sW)}{(s_1^2 - s^2)^2} ds \tag{34}$$

In order to determine β it is necessary to evaluate the integral in s-space on the right hand side of (34). Despite initial appearances the integrand is non-singular at $s = s_1$, taking a finite value at this point. There is, however, a genuine singularity when the denominator of Γ becomes zero. This only occurs when the outer slab is not cut-off and possesses a slab propagation constant β_0. The outer slab is the planar structure lying outside the vertical layers either side of the rib. However, β for the rib waveguide is known to lie above β_0 and thus the problem of this singularity is overcome by setting β_0 as a lower limit in the searching procedure.

The simplest way to evaluate the integral is numerically. Satisfactory results are obtained by using, say, the trapezium sum rule. The integrand decays rapidly as s^{-3} making this task easier. Simplifications such as exploiting symmetry in s, storing values of expressions which do not depend on β in arrays, and making use of the periodic form of $\cos(sW)$ all help to optimize this procedure. Incidentally, other evaluation techniques such as one involving a combination of a series

summation and an asymptotic expansion can also be equally successful (see McIlroy, chapter 5 in [7).

Roots to the determinantal equation can be found by stepping down systematically in values of β until a root is bracketed. Then either, say, the bisection method or Newton's method [27], with numerical differentiation, can be employed to determine β to the required accuracy.

Field profiles can be obtained once β has been determined. The procedure is straightforward in the rib and cladding as β is merely substituted back into (12) for the rib and the field is, of course, zero in the cladding. Below the rib the transformed field profile must be converted back into real space. This can be done efficiently by implementing a Fast Fourier Transform (FFT) algorithm [27].

Equation (34) yields the propagation constants of the even modes supported by the waveguide. For odd modes we return to (9) and replace it with

$$F(x) = \sin(s_1 x) \tag{35}$$

with s_1 now defined as π/W. Following through the analysis we obtain a similar transcendental equation for β except that $\cos^2(sW)$ is now replaced by $\sin^2(sW)$ in (34). Furthermore, propagation constants for any higher order modes (either even or odd) can be found by searching in value below that of the lowest order mode.

Although a simple rib waveguide has been discussed here, the SI method can be applied to structures with any number of layers both in and below the rib. For a multilayered rib some care must be taken when implementing the method of false position. Also, the left hand side of (21) must now be derived by linking the field solutions at all the dielectric interfaces. Similarly the expression for Γ can encompass additional layers. The greater the number of layers the more involved will these expressions become. Thus for multilayered structures this procedure is incorporated as part of the computational process using the cascade process [28] or response function technique [29].

2.5 Results

New waveguide modeling techniques and improvements to existing techniques are continually being developed. In order to compare one technique with another a selection of bench-mark structures have

emerged. Here we use four such structures (referred to in the literature as BT1, BT2, BT3 and UCL2 and originally considered in [13] and [30]) and compare computed values of modal index (β/k_0) obtained by the SI method with those obtained by the semi-vectorial finite difference (SVFD) method [10],[12]. The SVFD method was chosen as it is a well-established, highly accurate technique.

The dimensions of the four structures are listed in Table 1 using the notation of Figure 2. For BT1, BT2 and BT3 the operational wavelength is $1.55\mu m$ whereas for UCL2 the operational wavelength is $1.15\mu m$. In Table 2 we present modal index β/k_0 calculated for structures BT1, BT2 and BT3 for the fundamental quasi-TE mode. Similar results are presented in Table 3 but for the fundamental quasi-TM mode. In Table 4 we present values for β/k_0 for structure UCL2 for both the lowest-order even and lowest-order odd mode and for both polarizations. In all cases the difference in value between the modal indices calculated by the two methods and the corresponding percentage difference are tabulated.

structure	n_1	n_2	n_3	$2W(\mu m)$	$h(\mu m)$	$d(\mu m)$
BT1	1.00	3.44	3.34	2.0	1.1	0.2
BT2	1.00	3.44	3.36	3.0	0.1	0.9
BT3	1.00	3.44	3.435	4.0	2.5	3.5
UCL2	1.00	3.4406	3.4145	14.0	0.5	1.0

Table 1. Parameters for structures BT1, BT2, BT3 and UCL2 using the notation of Figure 2.

structure	SI	SVFD	SI-SVFD	% diff.
BT1	3.38874	3.38826	$+4.8 \times 10^{-4}$	+0.0142
BT2	3.39506	3.39521	-1.5×10^{-4}	-0.0046
BT3	3.43688	3.43681	$+7 \times 10^{-5}$	+0.0021

Table 2. Values of β/k_0 for the fundamental quasi-TE mode for structures BT1, BT2 and BT3 (see Table 1) calculated using the SI = spectral index method and SVFD = semi-vectorial finite difference method [12], together with the difference and percentage difference between the 2 values in each case.

structure	SI	SVFD	SI-SVFD	% diff.
BT1	3.38788	3.38754	$+3.4 \times 10^{-4}$	+0.0100
BT2	3.39032	3.39057	-2.5×10^{-4}	-0.0074
BT3	3.43684	3.43678	$+6 \times 10^{-5}$	+0.0017

Table 3. Values of β/k_0 for the fundamental quasi-TM mode. Other details are as for Table 2.

structure	SI	SVFD	SI-SVFD	% diff.
TE/even	3.42870	3.342877	-7×10^{-5}	+0.0020
TM/even	3.42807	3.42809	-2×10^{-5}	-0.0006
TE/odd	3.42804	3.42814	-1.0×10^{-4}	+0.0029
TM/odd	3.42741	3.42746	-5×10^{-5}	+0.0015

Table 4. Values of β/k_0 for structure UCL2 (see Table 1) for both the lowest-order even and lowest-order odd mode and for both quasi-TE and quasi-TM polarizations. Values calculated using the SI = spectral index method and SVFD = semi-vectorial finite difference method [10]. Also tabulated are the difference and percentage difference between the 2 values in each case.

Despite the wide variety of dimensions and refractive indices considered in these structures, the agreement between the two methods is close in all cases. The maximum percentage difference is only 0.01% while the closest result corresponds to a discrepancy of only 0.0006%

Some examples of field profiles calculated by the SI method for these structures are provided in Figure 4.

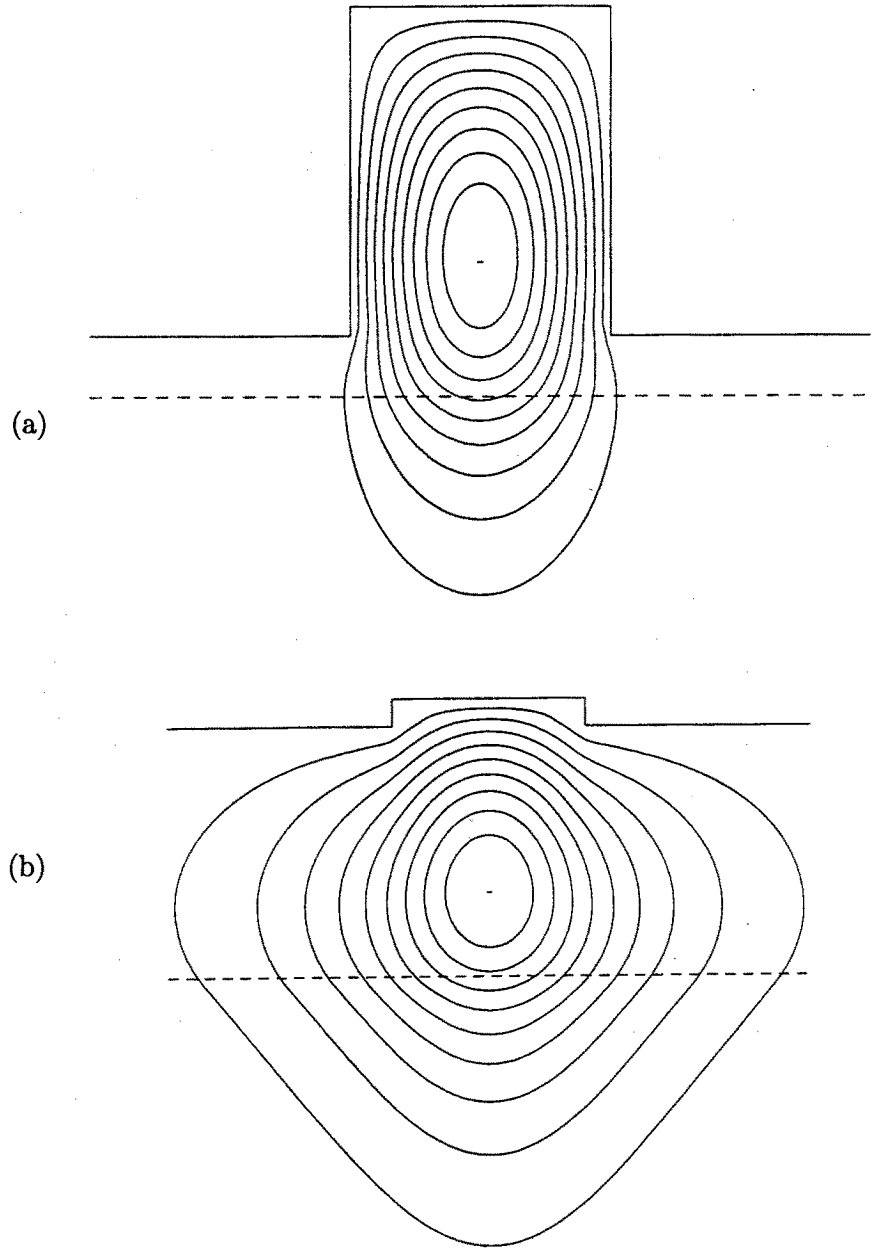

Figure 4. Field amplitude contours for the lowest-order quasi-TE mode at intervals of 10% for structures: (a) BT1 (b) BT2. See Table 1 and text for details.

(c)

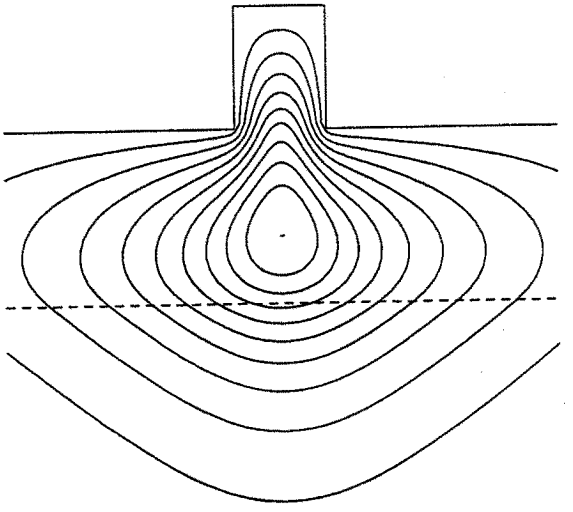

Figure 4. Field amplitude contours for the lowest-order quasi-TE mode at intervals of 10% for structures: (c) BT3. See Table 1 and text for details.

3. The Directional Coupler

Directional couplers consist of two adjacent parallel waveguides and form the basis of numerous optoelectronic devices, for example, polarization and wavelength filters, switches and modulators, power dividers and combiners. In the first part of this section we are interested in symmetric couplers where the two waveguides are identical. Light on entering one arm of a symmetric coupler periodically transfers to the opposite arm after a characteristic distance known as the coupling length L_c [31,32]. An accurate prediction of L_c is critical when designing a coupler device. L_c is defined by

$$L_c = \frac{\pi}{(\beta_s - \beta_a)} \tag{36}$$

and is generally short for weakly guiding or closely separated guides. Here, β_s and β_a are the propagation constants of the lowest-order symmetric and antisymmetric supermodes supported by the combined structure .

It is often necessary when designing a coupler device to make repeated calculations for example at a range of wavelengths or to optimize a device geometry. A method which can produce β_s and β_a rapidly but accurately is thus essential to this process. The SI method has proved ideal in this respect and indeed an early indication of the power of the SI method was its successful application to directional couplers [16–17] (see also Burke, chapter 7 in [7]). The analysis is very similar to that discussed already for the single rib waveguide, and is described below.

The structure is illustrated in Figure 5. It differs from the single rib waveguide illustrated in Figures 2 and 3 only in the presence of a second identical rib. The rib centers are separated by a distance $2L$. The boundaries with the cladding are again transposed using (4) and (5); the origin in this case is placed midway between the rib centers on the displaced semiconductor/air interface.

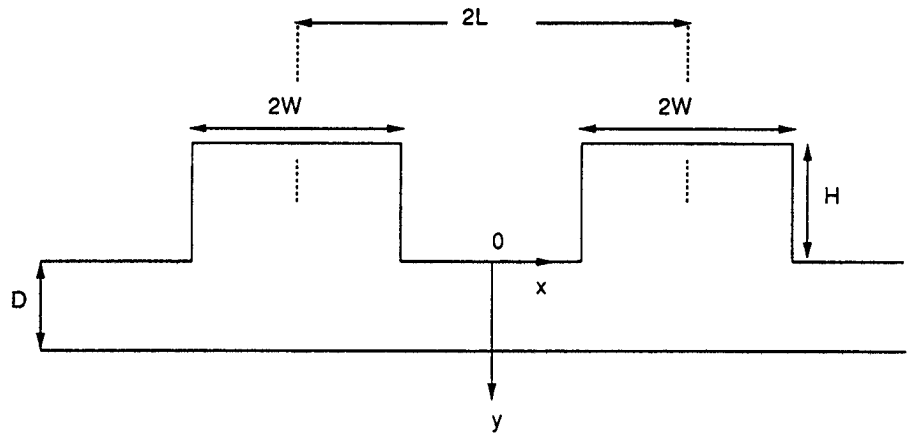

Figure 5. Cross-section through a symmetric rib waveguide directional coupler. Configuration has been transposed using the method of false position producing effective dimensions W, H and D.

For analysis the structure is divided along a line coincident with the transposed bases of the ribs. This results in a layered region below which is unchanged despite the addition of a second rib. Thus there remains only how to include the second rib and how to match it to the solution already derived.

Using the variational boundary condition (20) and letting ψ tend to zero we can write down for the symmetric coupler

$$\int_{-L-W}^{-L+W} E_-^*(\partial E/\partial y)_- dx + \int_{L-W}^{L+W} E_-^*(\partial E/\partial y)_- dx = \frac{1}{2\pi}\int_{-\infty}^{+\infty} \Gamma\phi_+\phi_+^* ds \tag{37}$$

Γ is defined in (27) and (30) and is unchanged in form for this case. The left hand side of (37) is constructed in the ribs as follows. We begin by choosing a separable solution $E = F(x)G(y)$ for each rib individually so that

$$E = A_1 G(y)\cos\{s_1(x+L)\} \qquad (-L-W) < x < (-L+W) \tag{38}$$

and

$$E = A_2 G(y)\cos\{s_1(x-L)\} \qquad (L-W) < x < (L+W) \tag{39}$$

Here, s_1 and $G(y)$ are defined as before and A_1 and A_2 are coefficients. For the lowest-order symmetric supermode we can set

$$A_1 = A_2$$

and for the lowest-order antisymmetric supermode we can set

$$A_1 = -A_2$$

Thus using (38) and (39) and their derivatives evaluated at $y = 0$, the two integrals on the left hand side of (37) can be evaluated analytically; both yield the same result, $A_1^2 W\gamma_1 \cot(\gamma_1 H)$.

As in our earlier analysis for the single rib waveguide, we take the Fourier transform of E evaluated at $y = 0$. In this case we have

$$\begin{aligned}\phi_- =& A_1 \int_{-L-W}^{-L+W} \cos\{s_1(x+L)\}\, e^{jsx} dx \\ &+ A_2 \int_{L-W}^{L+W} \cos\{s_1(x-L)\}\, e^{jsx} dx\end{aligned} \tag{40}$$

Choosing the symmetric form $\cos(sx)$ of e^{jsx} for the symmetric supermode we find

$$\phi_- = 4A_1 \cos(sW)\cos(Ls)\frac{s_1}{(s_1^2 - s^2)} \tag{41}$$

and similarly choosing the antisymmetric form $j\sin(sx)$ of e^{jsx} for the antisymmetric supermode we find

$$\phi_- = -4jA_1 \cos(sW)\sin(Ls)\frac{s_1}{(s_1^2 - s^2)} \tag{42}$$

Either (41) or (42) is then substituted into (37) along with our previous result for the left hand side. We see that A_1 cancels on both sides and we are left with the transcendental equation for the symmetric directional coupler:

$$\gamma_1 \cot(\gamma_1 H) = \frac{4s_1^2}{\pi W}\int_{-\infty}^{+\infty} \frac{\Gamma \cos^2(Ws)}{(s_1^2 - s^2)^2} \begin{Bmatrix} \cos^2(Ls) \\ \\ \sin^2(Ls) \end{Bmatrix} ds \tag{43}$$

The upper and lower form of (43) yield β_s and β_a respectively. The integral in (43) can be evaluated numerically with no difficulty using similar techniques to those discussed in section 2.

3.1 Results

In this section we compare calculated values of coupling length L_c obtained using the SI method, the semi-vectorial finite difference (SVFD) method [10–12], the finite element (FE) method (calculated by ETHZ - Besse, Swiss Federal Institute of Technology) and the effective index (EI) method [14] for an InP/InGaAsP strip-loaded symmetric coupler [33–35] whose dimensions and indices are illustrated in Figure 6. The height of the ribs is assumed large enough so as not to influence the results and the operational wavelength is $1.55\mu m$.

Figure 7 is a plot of percentage difference in L_c between the value obtained by the FE method and that obtained by each of the three remaining methods, for a range of rib separations t from $1\mu m$ to $4\mu m$ and for quasi-TE modes. As can be clearly seen the SI results are in close agreement with those produced by the two large-scale numerical methods across the whole range of rib separations.

Examples of calculated field profiles are shown in Figure 8 for the TE lowest-order symmetric mode for the structure in Figure 6 and for values of t of $1\mu m$ and $4\mu m$.

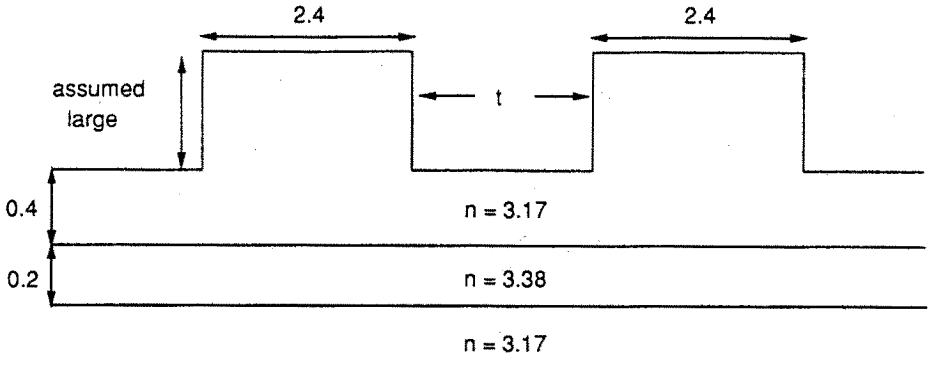

Figure 6. Cross-section through an InP/InGaAsP ridge waveguide symmetric coupler. Dimensions are in μm.

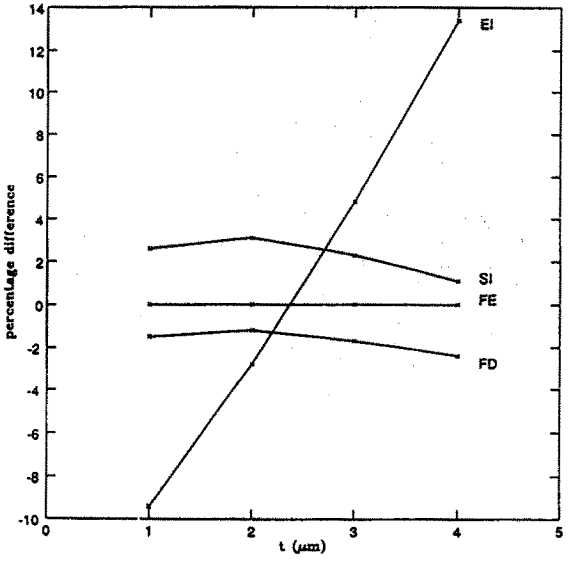

Figure 7. Comparison of coupling lengths calculated by SI (spectral index method), EI (effective index method) and FD (finite difference method) as a percentage difference from FE (finite element method).

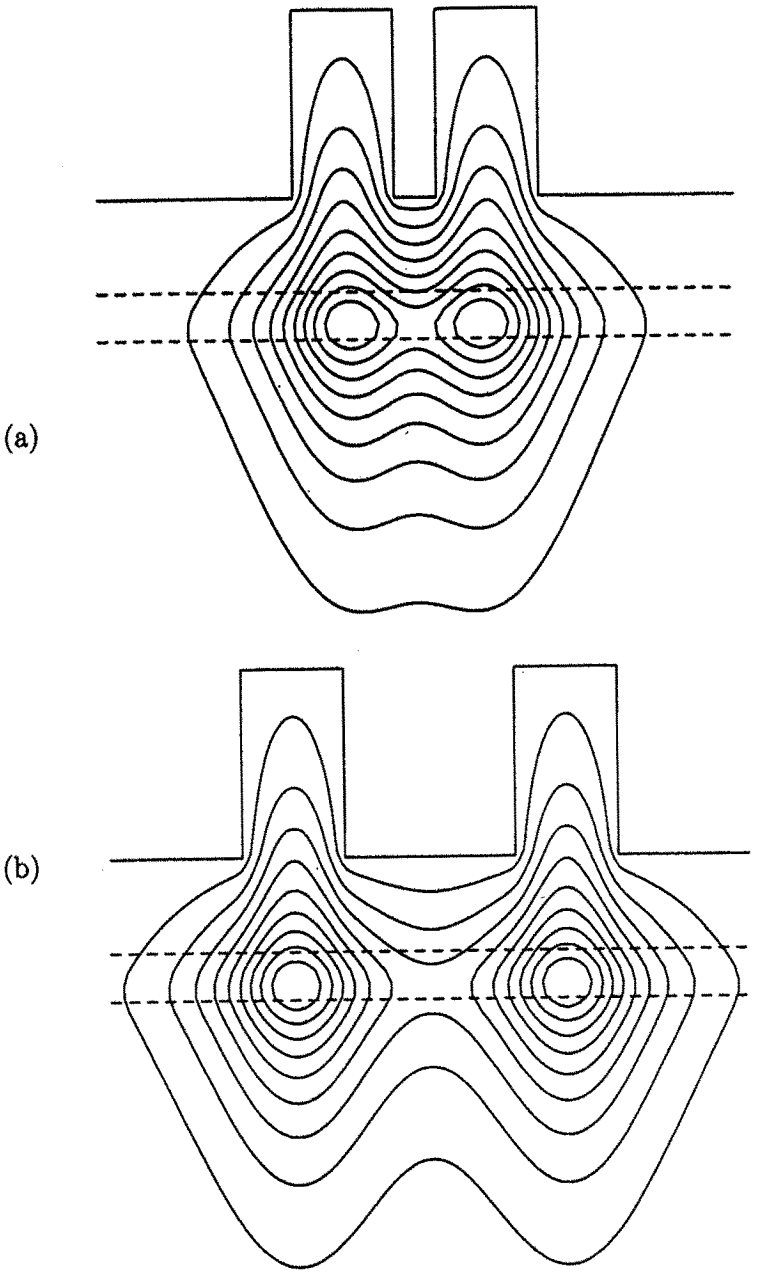

Figure 8. Field amplitude contours for the lowest-order quasi-TE symmetric supermode at intervals of 10% of maximum for the structure illustrated in Figure 6. Separation between the edges of the ribs, t = (a) $1.0\mu m$ and (b) $4.0\mu m$.

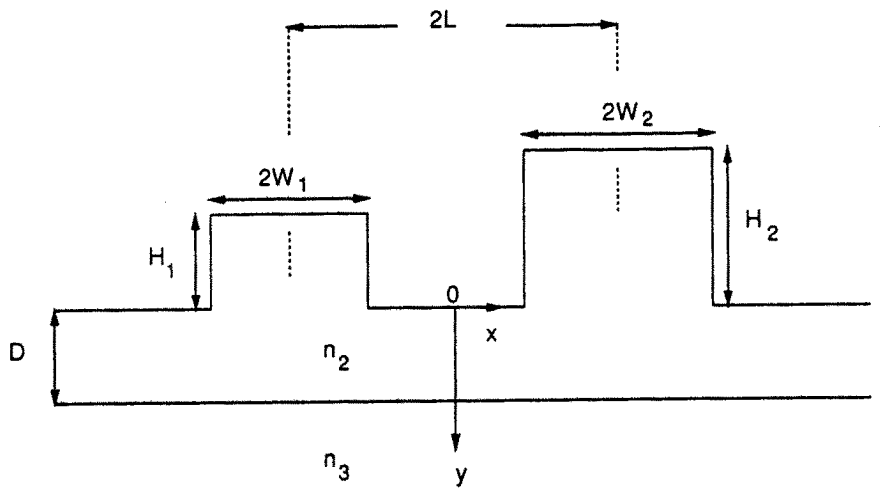

Figure 9. Cross-section through an asymmetric rib waveguide directional coupler. Dimensions shown are effective values following the application of the method of false position. The origin is placed midway between the rib centers on the displaced semiconductor/air boundary.

3.2 The Asymmetric Coupler

The SI method can also be applied to couplers where the ribs have different geometries (different heights and widths) and different composition (different number of layers and indices). Such an asymmetric coupler will generally support 2 lowest-order supermodes, if the two component guides when in isolation are single-moded, but the corresponding field profiles are typically concentrated in opposite guides [31,32]. Using the SI method, a transcendental equation can be constructed using the same fundamental principles. Only a brief description of the analysis is provided here but the reader is referred to [18] and Burke (chapter 7 in [7]) for a more comprehensive treatment. We consider an asymmetric rib waveguide coupler (Figure 9) where one rib has effective dimensions $2W_1$ and H_1 and the opposite rib has effective dimensions $2W_2$ and H_2.

We can write down the form of the variational expression for this case:

$$\int_{-L-W_1}^{-L+W_1} E_-^*(\partial E/\partial y)_- dx + \int_{L-W_2}^{L+W_2} E_-^*(\partial E/\partial y)_- dx$$
$$= \frac{1}{2\pi}\int_{-\infty}^{+\infty} \Gamma\phi_+\phi_+^* ds \tag{44}$$

To construct the left hand side of (44) we begin by selecting field expressions for the two ribs in the form

$$E = A_1 G_1(y)\cos\{s_1(x+L)\} \quad (-L-W_1) < x < (-L+W_1) \tag{45}$$
$$E = A_2 G_2(y)\cos\{s_2(x-L)\} \quad (L-W_2) < x < (L+W_2) \tag{46}$$

where $s_{1,2} = \pi/2W_{1,2}$,

$$G_{1,2} = \frac{\sin\gamma_{1,2}(y+H_{1,2})}{\sin\gamma_{1,2}H_{1,2}} \tag{47}$$

and $\gamma_{1,2} = (k_2^2 - s_{1,2}^2 - \beta^2)^{1/2}$.
Unlike the case of the symmetric coupler, there is no simple relationship between A_1 and A_2 and therefore both coefficients must be retained in the analysis. Determining E and $\partial E/\partial y$ at $y = 0$, and evaluating the two integrals, the left hand side LHS of (44) becomes

$$LHS = W_1 A_1^2 \gamma_1 \cot(\gamma_1 H_1) + W_2 A_2^2 \gamma_2 \cot(\gamma_2 H_2) \tag{48}$$

Looking now at the right hand side of (44) we note that Γ remains unchanged and has the form of (30). We now need to evaluate ϕ_+ by taking the Fourier transform of E just above the bases of the ribs. Due to the asymmetry of the problem, we must take both real and imaginary parts of the transform. After some algebra we find that the product $\phi_+\phi_+^*$ has the form

$$\phi_+\phi_+^* = A_1\alpha_1 + A_2\alpha_2 + 2A_1A_2\alpha_1\alpha_2\cos(2Ls) \tag{49}$$

where

$$\alpha_{1,2} = \frac{2\cos(W_{1,2}s)s_{1,2}}{(s_{1,2}^2 - s^2)} \tag{50}$$

Substituting (48), (49) and (50) into (44) we construct a transcendental equation for the asymmetric coupler. However, the two coefficients A_1 and A_2 still remain. Because of the variational nature of the SI method, we can eliminate both coefficients by first differentiating with respect to each in turn, setting the resultant pair of expressions to zero and then solving the two simultaneous equations. In this way we construct a transcendental equation independent of the coefficients:

$$\left[W_1\gamma_1\cot(\gamma_1 H_1) - \frac{1}{2\pi}\int_{-\infty}^{+\infty}\Gamma\alpha_1^2 ds\right]\left[W_2\gamma_2\cot(\gamma_2 H_2) - \frac{1}{2\pi}\int_{-\infty}^{+\infty}\Gamma\alpha_2^2 ds\right]$$
$$= \left[\frac{1}{2\pi}\int_{-\infty}^{+\infty}\Gamma\alpha_1\alpha_2\cos(2Ls)ds\right]^2 \tag{51}$$

Equation (51) yields both β_s and β_a. As can be seen three integrals must be evaluated. However, the 2 integrals on the left hand side of (51) are identical in form to those corresponding to both guides when in isolation and the third integral poses no additional problems. For the case $\alpha_1 = \alpha_2$, (51) reduces to (43), the transcendental equation for the symmetric coupler, as expected.

For most problems it is quite adequate to select only the leading term in the Fourier series (see (7)) in each rib as we have done here. However, situations can arise when one rib is much wider than the other and then an additional term may need to be taken in this rib. In this case, the same procedure applies but 3 rather than 2 coefficients will be involved, yielding 3 simultaneous equations and resulting in a more complicated but still manageable transcendental equation [18].

4. The Discrete Spectral Index Method

The discrete spectral index (DSI) [25] (also Stern, chapter 6 in [7]) method is an alternative form of the standard SI method. Instead of taking the Fourier transform of the field in the layered region below the rib(s), we now express the field as a Fourier series in real space. We

assume the field to occupy a finite width in x with the field vanishing at $x = 0$ and $2T$ (see Figure 10), where we have assumed for simplicity the origin to be on the left hand boundary. We then express the field in the form:

$$E(x, y) = \sum_{q=1}^{\infty} G_q(y) \sin(s_q x) \tag{52}$$

Here, G_q represents slab-like field expressions of similar form to (17) and (18). Thus

$$G_q(y) = A_q \sin\{\Gamma_2(y - D)\} + B_q \cos\{\Gamma_2(y - D)\} \qquad 0 < y < D \tag{53}$$

$$G_q(y) = C_q \exp\{-\Gamma_3(y - D)\} \qquad y > D \tag{54}$$

where A_q, B_q and C_q are coefficients. Γ_2 and Γ_3 have the same form as before but now $s_q = q\pi/2T$ replaces the spatial spectral variable, s.

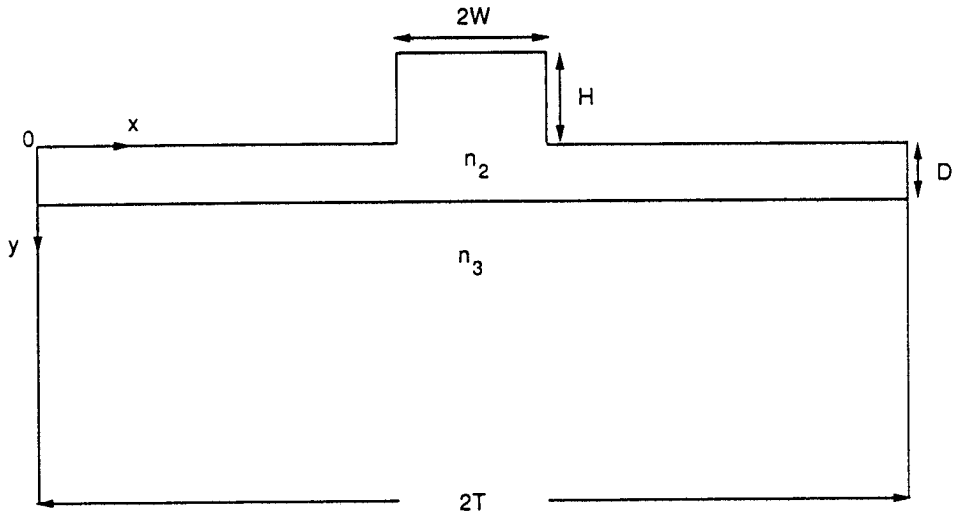

Figure 10. Structure and coordinate system of a rib waveguide for analysis by the discrete SI method. Dimensions shown are effective values.

We employ the variational boundary condition of (20). For a single rib waveguide we can write

$$\gamma_1 W \cot(\gamma_1 H) = T \sum_{q=1}^{\infty} G_q^2(0) \Gamma_q \tag{55}$$

The left hand side of (55) is constructed in the rib and has the same form as that derived for the traditional SI method. On the right hand side, constructed below the rib, the integral in x has been evaluated and is just T. Γ_q is given by

$$\Gamma_q = \frac{dG_q(0)/dy}{G_q(0)} \tag{56}$$

which has the form of Γ in (30) but now s_q replaces s. $G_q(0)$ in (55) is determined by equating field expressions across the base of the rib (at $y = 0$) and applying standard orthogonality properties of Fourier series over the interval $x = 0$ to $2T$. Thus for even modes

$$\int_{T-W}^{T+W} \cos(s_1(x-T)) \sin(s_q x) dx = G_q(0) \int_0^{2T} \sin^2(s_q x) dx \tag{57}$$

for a given q. After evaluating both integrals (57) becomes

$$\frac{2s_1 \cos(s_q W)}{(s_1^2 - s_q^2)} = T G_q(0) \tag{58}$$

We can now substitute $G_q(0)$ from (58) into (55) to obtain the required transcendental equation for this case:

$$\gamma_1 \cot(\gamma_1 H) = \frac{4s_1^2}{WT} \sum_{q=1}^{\infty} \frac{\Gamma_q \cos^2(s_q W)}{(s_1^2 - s_q^2)^2} \tag{59}$$

Care must be taken to ensure that a large enough value of T is selected and similarly that enough terms are chosen for the summation in (59). T must be increased for weakly guiding structures; the larger the value of T the more terms are required for convergence. If we allow T to tend to infinity the DSI method becomes equivalent to the original SI method. Identical results can of course be obtained using the two approaches. The DSI method, however, has the advantage

of being conceptually simpler. Also, using the DSI method overlap integrals between two modes can be obtained in an extremely efficient way. This is the subject of our next section.

4.1 Overlap Integrals

When modeling waveguide devices it is often useful to know the value of the overlap integral for a particular pair of modes. The overlap integral is the product of two field profiles summed over the cross-sectional area of the structure. For example, an overlap integral between the supermodes supported by a coupler and the mode supported by one isolated arm can yield important information on the insertion loss occurring at the output. Alternatively, the light propagation through a tapered coupler, where the separation between the ribs is slowly varied, can be modeled by representing the structure as a series of short parallel sections and performing overlap integrals between the two pairs of supermodes at each interface [22].

Normally to evaluate an overlap integral it is necessary to define a mesh and generate field values for each mode at each mesh point before integrating numerically. Using the DSI method this procedure is necessary only for the relatively small areas within the ribs. (If the ribs corresponding to the two modes involved coincide, the overlap integral can be evaluated analytically here.) Below the rib, because the field is described in terms of a Fourier series, the calculations can be performed entirely in Fourier space. This results in a highly efficient procedure. The methodology is described below.

Let E_1 and E_2 be the fields below the ribs corresponding to any two modes so that using the DSI method, see (52), we can write

$$E_1 = \sum_{q=1}^{\infty} G_q^I(y) \sin(s_q x) \tag{60}$$

$$E_2 = \sum_{q=1}^{\infty} G_q^{II}(y) \sin(s_q x) \tag{61}$$

The superscripts I and II refer to modes 1 and 2 respectively. The overlap integral $\sum_{12}$ between these modes is given by

$$\sum\nolimits_{12} = \int_0^{2T} \int_0^{\infty} E_1 E_2 dy dx \tag{62}$$

or

$$\sum_{12} = T \sum_{q=1}^{\infty} \int_0^{\infty} G_q^I(y) G_q^{II}(y) dy \tag{63}$$

after evaluating the integral in x. Both $G_q^I(y)$ and $G_q^{II}(y)$ independently satisfy wave equations so that

$$\frac{d^2 G_q^I(y)}{dy^2} + (k^2(y) - \beta_1^2 - s_q^2) G_q^I(y) = 0 \tag{64}$$

where β_1 is the propagation constant of mode 1. A similar expression can be written down for $G_q^{II}(y)$ but with β_2 replacing β_1. If we multiply (64) by $G_q^{II}(y)$, and multiply the corresponding equation for $G_q^{II}(y)$ by $G_q^I(y)$, integrate over all y and subtract one expression from the other noting that $G_q^I(y)$ and $G_q^{II}(y)$ vanish at infinity we can write

$$\begin{aligned} &G_q^I(0) dG_q^I(0)/dy - G_q^{II}(0) dG_q^{II}(0)/dy \\ &= (\beta_1^2 - \beta_2^2) \int_0^{\infty} G_q^I(y) G_q^{II}(y) dy \end{aligned} \tag{65}$$

If we define Γ as in (56) with the appropriate β for either mode and substitute (65) into (63) we obtain the required expression for the overlap integral between 2 modes

$$\sum_{12} = \frac{T \sum_{q=1}^{\infty} G_q^I(0) G_q^{II}(0) \{\Gamma_q^I - \Gamma_q^{II}\}}{(\beta_1^2 - \beta_2^2)} \tag{66}$$

We see immediately from (66) that for each overlap integral only one summation is required and there is no need to integrate over y. For normalization purposes we also require E_1^2 and E_2^2 integrated over all space. To do this we use (63) with $G_q^I(y) = G_q^{II}(y)$. The integral in y can be evaluated analytically for each layer.

5. Complex Form of the SI Method

The discussion so far in this chapter refers to waveguides for which the refractive indices concerned are assumed to be real. However, many devices of interest in optoelectronics have metal layers [36], or experience gain or loss which results in complex refractive indices and therefore complex propagation constants [37]. It has been shown recently that the SI method can be generalized to include the analysis of such complex structures [19]. In fact, the transcendental equations for, for example, the single rib waveguide, symmetric or asymmetric coupler still apply. They retain their algebraic form, but become complex, with real refractive indices replaced by complex ones. For confirmation of this result, we refer to Oksanen and Lindell in [38] who prove that this is so provided the variational functional can be differentiated in the complex plane in a region surrounding the stationary point. Also, any additional complex notation introduced by for example the spatial Fourier transform must be kept separate. (See also Jones, chapter 3 in [7] and [39]).

Searching for β in the complex plane can be a rather precarious process. One approach that has proved successful for the SI method uses a combination of the method of embedding described in [40] for slab waveguides and Newton's method. We write the dielectric constant $\varepsilon(=\varepsilon_0 n^2)$ of each layer in terms of its real (ε_r) and imaginary (ε_i) parts in the form

$$\varepsilon = \varepsilon_r + i\varepsilon_i \frac{p}{p_{\max}} \tag{67}$$

where $p_{\max}$ is an integer say 5 and $p = 0, 1, 2, \ldots p_{\max}$. We then solve for β with p initially equal to zero. This initial problem is real, and is thus easily solved by first bracketing the root and then using Newton's method in the form

$$\beta_{q+1} = \beta_q - \frac{2F(\beta_q)\Delta}{F(\beta_q + \Delta) - F(\beta_q - \Delta)} \tag{68}$$

where Δ is a small, real number. We then set $p = 1$ so the problem becomes complex and solve for β again, now also complex, using Newton's method with β from the previous iteration as our initial guess. In (68) Δ remains real. This process is repeated until $p = p_{\max}$.

6. Summary

The Spectral Index (SI) method is a semi-analytical technique which analyses semiconductor rib and related waveguides in a novel way. The scalar wave equation is solved and a transcendental equation is constructed from which the propagation constants of the guided modes can be determined numerically. The SI method is efficient in terms of CPU time and storage and yields propagation constants, coupling lengths and field profiles in favorable agreement with established, accurate techniques. The SI method has been extended to model symmetric couplers, asymmetric couplers and waveguides incorporating gain or loss. The SI method is now firmly established as a powerful design tool for a wide range of optoelectronic devices.

References

1. Kendall, P. C., P. W. A. McIlroy, and M. S. Stern, "Spectral index method for rib waveguide analysis," *Electron. Lett,* Vol. 25, 107–108, 1989.
2. Kendall, P. C., P. W. A. McIlroy, and M. S. Stern, "Analysis of semiconductor rib waveguides: spectral index method," *IEE Colloquium on Integrated Optics, IEE Digest,* 13/1–13/4, 1989/93.
3. McIlroy, P. W. A., M. S. Stern, and P. C. Kendall, "Fast and accurate method for calculation of polarized modes in semiconductor rib waveguides," *Electron. Lett.,* Vol. 25, 1586–1587, 1989.
4. Hewson-Browne, R. C. and P. C. Kendall, "Note on optoelectronic propagation using spectral index technique," *Electron. Lett.,* Vol. 25, 1153–1154, 1989.
5. McIlroy, P. W. A., M. S. Stern, and P. C. Kendall, "Spectral index method for polarized modes in semiconductor rib waveguides," *IEEE J. Lightwave Technol.,* Vol. LT-8, 113–117, 1990.
6. Stern, M. S., P. C. Kendall, and P. W. A. McIlroy, "Analysis of the spectral index method for vector modes of rib waveguides," *IEE Proc.,* Vol. 137, Pt. J, 21–26, 1990.
7. Robson, P. N., and P. C. Kendall (Eds.), *Rib Waveguide Theory by the Spectral Index Method,* Research Studies Press and Wiley, 1990.

8. Vassallo, C., and Y. H. Wang , "A new semirigorous analysis of rib waveguides," *IEEE J. Lightwave Technol.*, Vol. LT-8, 56–65, 1990.
9. Vassallo, C., *Optical Waveguide Concepts,* Elsevier, 1991.
10. Stern, M. S., "Semivectorial polarized finite difference method for optical waveguides with arbitrary index profiles," *IEE Proc.*, Vol. 135, Pt. J, 56–63, 1988.
11. Stern, M. S., "Semivectorial polarized H field solution for dielectric waveguides with arbitrary index profiles," *IEE Proc.*, Vol. 135, Pt. J, 333–338, 1988.
12. Stern, M. S., "Rayleigh quotient solution of semivectorial field problems for optical waveguides with arbitrary index profiles," *IEE Proc.*, Vol. 138, Pt. J, 185–190, 1991.
13. Rahman, B. M. A., and J. B. Davies, "Vector-H finite element solution of GaAs/GaAlAs rib waveguides," *IEE Proc.*, Vol. 132, Pt. J, 349–353, 1986.
14. Knox, R. M., and , P. P. Toulios, "Integrated circuits for the millimeter through optical frequency range," *in Fox, J. (Ed.), Proc. of MRI Symposium on Submillimeter Waves,* Polytechnic Press, 497–518, 1970.
15. Kendall, P. C., M. J. Adams, S. Ritchie, and M. J. Robertson, "A theory for calculating approximate values for the propagation constants of an optical rib waveguide by weighting the refractive indices," *IEE Proc.*, Vol. 134, Pt. A, 699–702, 1987.
16. Burke, S. V., "Spectral index method applied to coupled rib waveguides," *Electron. Lett.*, Vol. 25, 605–606, 1989.
17. Burke, S. V., "Spectral index method applied to rib and strip-loaded directional couplers," *IEE Proc.*, Vol. 137, Pt. J, 7–10, 1990.
18. Burke, S. V., "Spectral index method applied to two nonidentical closely separated rib waveguides," *IEE Proc.*, Vol. 137, Pt. J, 289–292, 1990.
19. Burke, S. V., "Novel semianalytic rib/ridge semiconductor waveguide design including gain and loss," *Electron.Lett.*, Vol. 28, 2280–2282, 1992.
20. Burke, S. V., "Analysis of a novel rib waveguide wavelength filter by the spectral index method," *Technical Digest on Integrated Photonics Research,* Vol. 5, 86–87, 1990.

21. Burke, S. V., and P. C. Kendall, "Analysis of a rib waveguide filter response with variable separation," *Technical Digest on Integrated Photonics Research,* Vol. 8, 117, 1991.
22. Burke, S. V., P. C. Kendall, S. Ritchie, M. J. Robertson, and P. N. Robson, "Analysis of rib waveguide coupler filters," *IEE Proc.,* Vol. 139, Pt. J, 59–65, 1992.
23. Burke, S. V., M. J. Adams, P. C. Kendall, P. N. Robson, and G. J. Rees, "Design of ridge waveguide couplers with carrier injection using the discrete spectral index method," *Electron. Lett.,* Vol. 28, 841–843, 1992.
24. Burke, S. V., M. J. Adams, P. C. Kendall, P. N. Robson, and G. J. Rees, "Application of the discrete spectral index method to the design of coupled ridge waveguides with carrier injection," *Technical Digest on Integrated Photonics Research,* Vol. 10, 170–171, 1992.
25. Kendall, P. C., M. S. Stern, and P. N. Robson, "Discrete spectral index method for rib waveguide analysis," *Optical and Quantum Electronics,* Vol. 22, 555–560, 1990.
26. Ramo, S., J. R. Whinnery, and T. Van Duzer, *Fields and Waves in Communication Electronics,* (2nd Ed.), Wiley, 1984.
27. Press, W. H., B. P. Flannery, S. A. Teukolsky, and W. T. Vetterling, *Numerical Recipes: The Art of Scientific Computing,* Cambridge University Press, 1992.
28. Collin, R. E., *Field Theory of Guided Waves,* (2nd Ed.), IEEE Press, 188–189, 1991.
29. Wait, J. R., *Electromagnetic Waves in Stratified Media,* (2nd Ed.), Pergamon Press, 1970.
30. Robertson, M. J., S. Ritchie, and P. Dayan, "Semiconductor waveguides: analysis of optical propagation in single rib structures and directional couplers," *IEE Proc.,* Vol. 132, Pt. J., 336–342, 1985.
31. Haus, H. A., *Waves and Fields in Optoelectronics,* Prentice-Hall, 1984.
32. Marcuse, D., *Theory of Dielectric Optical Waveguides,* (2nd Ed.), Academic Press, 1991.
33. Lagasse, P., et al, "COST-216 comparative study of eigenmode analysis methods for single and coupled integrated optical waveguides," *IEE European Conference on Optical Communications,* No. 292, 296–299, 1988.

34. Working Group 1, COST 216, "Comparison of different modeling techniques for longitudinally invariant integrated optical waveguides," *IEE Proc.*, Vol. 136, Pt. J, 273–280, 1989.
35. Mao, M, and W. P. Huang, "Analysis of optical rib waveguides and couplers with buried guiding layer," *IEEE J. Quantum Electron.*, Vol. QE-28, 176–183, 1992.
36. Albrecht, P., M. Hamacher, H. Heidrich, D. Hoffmann, H. P. Nolting, and C. M. Weinert, "TE/TM mode splitters on InGaAsP/InP," *IEEE Photon. Technol. Lett.*, Vol. 2, 114–115, 1990.
37. Buus, J., "The effective index method and its application to semiconductor lasers," *IEEE J. Quantum. Electron.*, Vol. QE-18, 1083–1089, 1982.
38. Oksanen, M. I., and I. V. Lindell, "Complex-valued functionals in variational analysis of waveguides with impedance boundaries," *IEE Proc.*, Vol. 136, Pt. H., 281–288, 1989.
39. Chen, C. H., and Y. W. Kiang, "The variational formulation of physical problems and the associated numerical techniques," in Kong, J. A., (Ed.), *Research Topics in Electromagnetic Wave Theory,* Wiley, 1981.
40. Sharma, E. K., M. P. Singh, and P. C. Kendall, "Exact multilayer waveguide design including absorbing or metal layers," *Electron. Lett.*, Vol. 27, 408–410, 1991.